GFRP-RC COLUMNS UNDER REVERSAL-CYCLIC LOADING

Mahmoud Ali[1] and Ehab El-Salakawy[2]

[1] M.Sc. Student, Dept. of Civil Eng., University of Manitoba, Winnipeg, MB, Canada
[2] Professor and CRC, Dept. of Civil Eng., University of Manitoba, Winnipeg, MB, Canada

Abstract: Using fiber reinforced polymers (FRP) reinforcement as main reinforcement in reinforced concrete (RC) structures becomes a viable solution to steel corrosion-related problems. Unlike steel, FRP bars do not yield, instead, they exhibit high tensile strength along with linear elastic behaviour up to failure. However, it is well-documented that the inelastic behaviour of steel in RC structures is common in dissipating earthquakes-induced energy. Accordingly, the performance of FRP-RC structures under seismic loading needs to be investigated. The objective of this research project is to study the effect of using glass (G) FRP longitudinal bars and stirrups on the performance of concrete columns under reversal cyclic loading. Two full-scale column prototypes, with 1650-mm long and 350-mm square cross-section, were constructed and tested under simulated seismic load conditions. The column specimen represented part of first storey column between the foundation and point of contra-flexure. The experimental results showed that both GFRP and steel columns were successfully able to sustain drift ratios higher than the values required by both the American Concrete Institute and the National Building Code of Canada. This indicates that the GFRP-RC columns can successfully sustain the gravity load in the presence of the seismic excitations.

1 INTRODUCTION

Engineering infrastructures are inherently vulnerable to steel corrosion, particularly for those subjected to de-icing salts and/or aggressive environments, leading to costly repair and rehabilitation as well as a significant reduction in service life. Noncorrosive Fiber reinforced polymers (FRP) reinforcement, as a substitute for internal steel reinforcing bars, has shown a promising performance in mitigating corrosion-related problems of steel reinforced concrete (R.C) structures. However, the elastic-linear behaviour of GFRP up to failure with low modulus of elasticity has raised concerns of the ability of GFRP reinforcement to replace steel reinforcement in earthquake-resistant structures, in which dissipation of earthquake-induced energy is mainly dependent on the nonlinear behaviour of their structural members. Therefore, the use of GFRP reinforcement in such members needs to be investigated.

To date, few available experimental studies have been carried out on GFRP-RC columns subjected to seismic loading. Sharbatdar et al. (2004) reported that columns reinforced internally with Carbon(C) FRP longitudinal bars and CFRP grids can be design to satisfy strength and deformability requirements of earthquake resistant structures. Tavassoli et al. (2015) concluded that columns reinforced with GFRP bars and spirals showed stable behaviour up to failure. Furthermore, the GFRP spirals delayed crushing of the concrete core, which increased the deformability of the columns.

2 DETAILS OF THE EXPERIMENTAL PROGRAM

2.1 Test Prototypes

The experimental study reported here is part of an ongoing experimental program in the McQuade Heavy Structures Laboratory at the University of Manitoba, in which full-scale square columns are constructed and tested under simulated seismic load. Test specimens simulate the lower portion of first storey columns between the footing and the contra-flexure point. As shown in Figure 1; the test specimens had a 350-mm square cross-section and a shear span of 1650-mm (distance between the footing and point of load application). These dimensions were chosen to promote flexure failure in addition to be representative of the columns commonly found in concrete structures.

In this paper; the test results and discussion will be presented for two specimens. First specimen (CS) was reinforced with steel bars and stirrups as a control specimen, while the second specimen (CG) was reinforced with GFRP bars and stirrups. The Canadian standards CSA A23.3-04 (CSA 2004) and CSA S806-12(CSA 2012) were used to design the two test specimens, respectively.

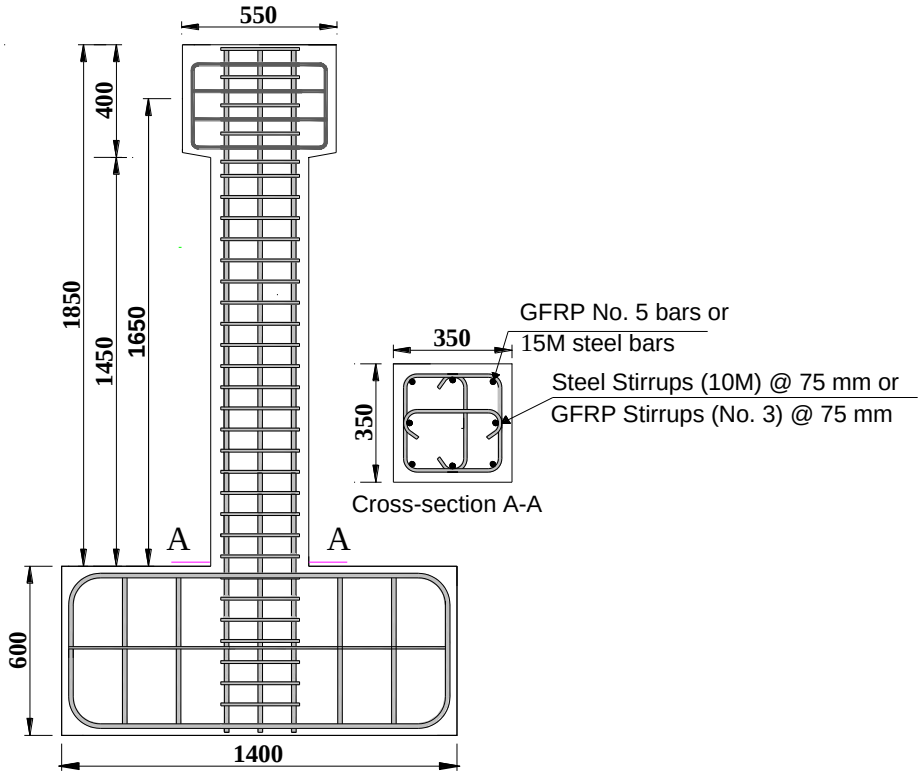

Figure 1: Dimensions and reinforcement details of the test specimens

2.2 **Materials**

All test specimens were constructed with normal-weight, ready-mixed concrete with a specified 28-day compressive strength of 35 MPa. The maximum nominal aggregate size was 19 mm, and the measured slump of the concrete was 120 mm. All test prototypes were cast and wet-cured in the laboratory for 7 days (Figure 2). The average concrete compressive strength was approximately 38.5 at the day of testing based on standard cylinder tests (152×305 mm). Two types of reinforcing bars were used in this study; CSA grade 400 deformed steel bars for specimen CS and sand-coated GFRP bars (Pultrall Inc. 2012) for specimen CG. The properties of the reinforcement as provided by the manufacturer are listed in Table 1.

2.3 Test setup and loading scheme

A heavily reinforced footing was fixed to the strong floor to provide rational fixity to the column. As shown in Figure 3; the simulated seismic load was applied using a 1000-kN fully dynamic actuator of ±250mm stroke. In addition, a hinged-loading frame was used to transfer the axial load from a 1000-kN capacity hydraulic jack to the column specimen and to allow translating the column laterally.

A load history consisted of a load-controlled phase followed by a displacement-controlled phase was applied to all test specimens. During the loading-controlled phase, two load cycles were applied, the first cycle was to reach the cracking load, and the second cycle represented the service loading condition for

both steel and GFRP(60% of the yielding strain in case of steel (CSA 2004) and 25% in case of the GFRP (CSA 2012).

Table 1: Properties of reinforcing bars

Bar Type	Bar diameter (mm)	Bar area (mm^2)	Modulus of elasticity (GPa)	Tensile strength (MPa)	Ultimate strain (%)
Steel					
16M	15.9	200	200	f_y= 400	ε_y= 0.2
10M	11.3	100	200	f_y= 400	ε_y= 0.2
GFRP Bars and Stirrups					
No.5	15.9	198	62	1184	1.89
No.3 [a]	9.5	71	52	1022	1.97

[a] Properties of the straight portion of the bent GFRP bar.

On the other hand; the displacement-controlled Phase was carried out according to the recommendation of the ACI Committee 374 Report on the acceptance criteria for moment frames based on structural testing (ACI 374.1 2005). In this phase, the load was applied at quasi-static rate of 0.01 HZ. Figure 4 shows the loading scheme, the numbers on top are the drift ratios (y-axis values), while the numbers on the X- axis are the cycle numbers.

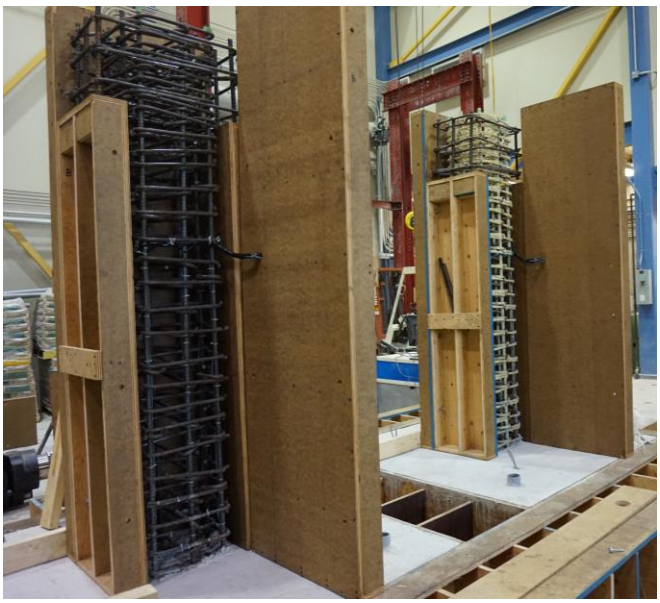

Figure 2: Construction process for the test specimens

Twenty electrical resistance strain gauges were attached to the reinforcing bars and stirrups to monitor strain variation at the critical locations. In addition, four linear variable displacement transducers (LVDTs)

were placed vertically near the critical section to measure the rotation of the column. All instrumentation was connected to a data accusation system to collect and record readings.

Figure 3: Test Set-up

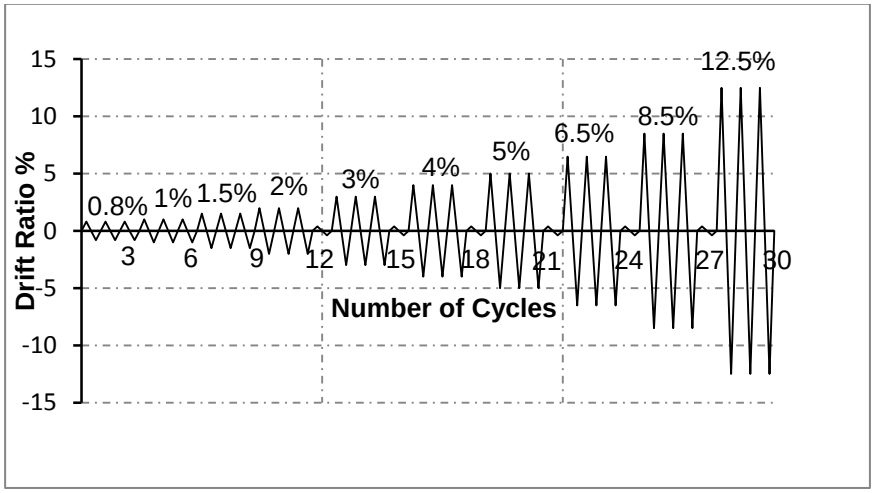

Figure 4: Seismic loading scheme

3 TEST RESULTS AND ANALYSIS

3.1 Crack Pattern and Mode of failure

Observations during testing indicate that specimen CS showed tiny flexure cracks during the 0.8% drift ratio. At 1% drift ratio, additional cracks were observed including a continuous crack at the column-footing interface as a result of the significant yield penetration into the footing. As the penetration depth increased, the crack at the column–footing interface propagated causing wider crack at the subsequent drift ratios. At 3% drift ratio; the concrete cover slightly started to spall off at the corner of the column and

more spalling of concrete was observed during the 4% drift ratio. At 5% drift ratio, concrete cover was completely spalled off, which resulted in exposing the reinforcement cage. Subsequently, the longitudinal bars started to buckle between the transverse reinforcement at the first cycle of the 6.5% drift ratio. When the column was forced to develop 8.5% drift ratio all the bars had ruptured after crushing of the concrete core.

For specimen CG, the observed behaviour during testing shows that flexure cracks appeared during the 0.8% drift ratio. In addition, a continuous crack appeared at the column-footing interface due to the elastic deformation of the bars inside the footing. The intensity of cracks increased from 1% to 2% drift ratio, which was uniformly distributed at the lower half of the column. Concrete cover started to spall off at 3% drift ratio at the compression side. At 5% drift ratio, the concrete cover was completely spalled off at the hinging region (the column segment from the footing up to a length equal to the side dimension of the column, approximately 350 mm) and the reinforcement cage was completely exposed. At the first cycle of the 12.5% drift ratio, crushing of the concrete core occurred followed by compression failure of the longitudinal bars between stirrups. Figure 5 shows photos of the two test specimens at failure.

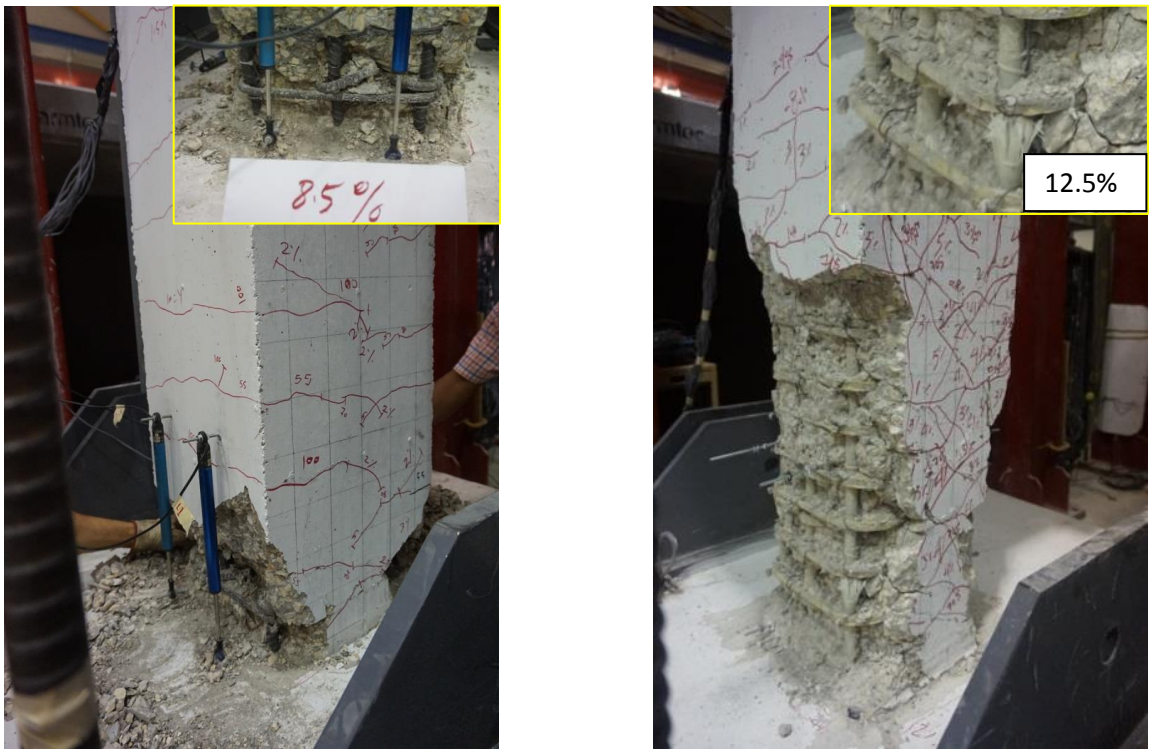

(a) Steel-RC specimen (CS)

(b) GFRP-RC specimen (CG)

Figure 5: Mode of failure of the tested specimens

3.2 Hysteresis Behaviour

The hysteresis diagram represents the relationship between the applied lateral load and the drift ratio of the column tip. The drift ratio was calculated as the horizontal displacement of the column divided by the unsupported height of the column. Figure 6 indicates that the hysteresis response of specimen CS showed gradual increase in the lateral resistance at the early loading stages. At 3% drift ratio, the maximum lateral capacity (147kN) was reached with a significant pinching of the hysteresis loop. At the subsequent loading steps, there was insignificant increase in the lateral capacity up to 5% drift ratio. Following the 5% drift ratio up to failure, there was a significant degradation in strength due to the deterioration of the concrete core.

For specimen CG, the hysteresis diagram shows different behaviour compared to specimen CS due to the different characteristics of the internal reinforcement. At the early stages of loading, specimen CG showed lower lateral resistance relative to specimen CS due to the relatively low modulus of elasticity of GFRP bars compared to steel. However, after 4%drift ratio, the lateral resistance of specimen CG exceeded the lateral resistance of specimen CS. Moreover, the maximum lateral resistance was developed at 8.5% (167 kN), while failure occurred at 12.5% drift ratio which resulted in an approximately 200% increase in the deformability with only 4% degradation in strength at failure. It can be noted that the descending portion of the hysteresis curve aimed approximately at the origin of the lateral load-drift relationship; as a result there was no significant pinching of the hysteresis loop.

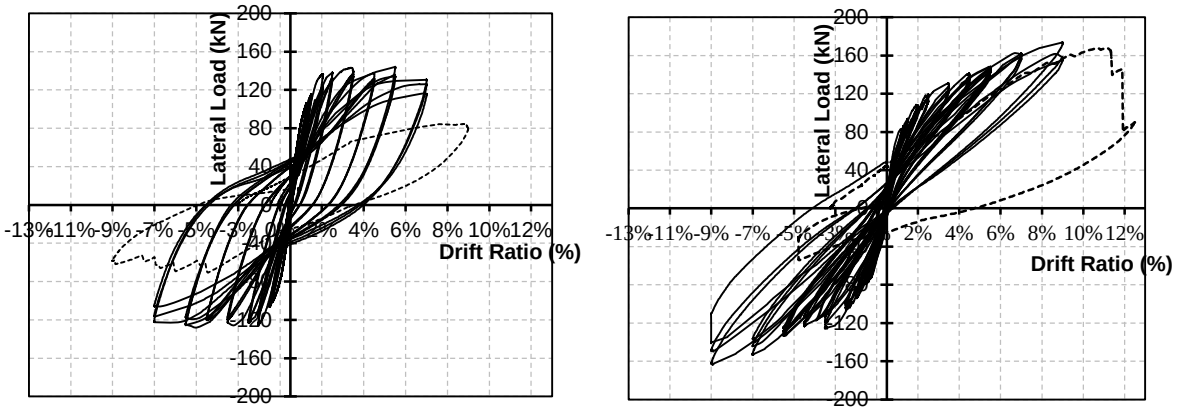

(a) Steel-RC specimen (CS) (b) GFRP-RC specimen (CG)

Figure 6: Hysteretic load-drift ratio relationship

3.3 Energy Dissipation

Figure 7 shows the cumulative energy dissipation of specimens CS and CG. The cumulative energy dissipation can be calculated by the total area under successful hysteresis loops. AS expected, Specimen CS showed higher energy dissipation than specimen CG due to the inelasticity of steel reinforcement after yielding which provides wider hysteresis loops. For example; the cumulative energy absorbed by steel reinforced specimen (CS) at 4% drift ratio was approximately 50 kN.m, while for CG it was approximately 22 kN.m.

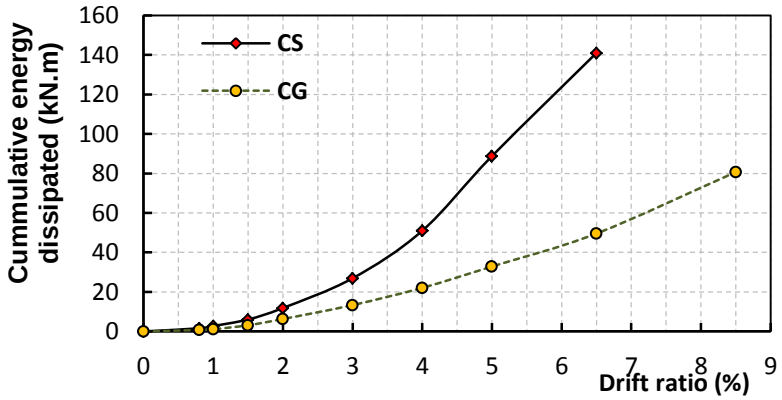

Figure 7: Cumulative energy dissipated by test specimens

4 CONCLUSIONS

Based on the results of the tested specimens, the following conclusions are drawn.

1- The GFRP-RC column showed stable behaviour when sustaining gravity load in the presence of the reversed-cyclic loading.
2- The drift capacity of steel as well as GFRP-RC specimen was more than the 2.5% and the 4% required by the National Building Code of Canada *(NBCC* 2010) and CSA/S806-12, respectively.
3- The cumulative energy absorbed by the GFRP-RC specimen during reversed-cyclic loading was approximately one-half that dissipated by steel-RC column.

5 ACKNOWLEDGEMENTS

The authors wish to express their gratitude and sincere appreciation for the financial support received from the Natural Science and Engineering Research Council of Canada, through Canada Research Chairs program and the Network of Centers of Excellence on Intelligent Sensing for Innovative Structures (ISIS Canada). The help received from the technical staff of the McQuade Heavy Structural Laboratory at the University of Manitoba is also acknowledged.

6 REFERENCES

ACI Committee 374. (2005). "Acceptance criteria for moment frames based on structural testing and commentary." ACI 374.1-05, American Concrete Institute, Farmington Hills, Detroit, 9 p.

Canadian Standards Association (CSA). (2004). "Design of concrete structures." CSA A23.3-04, Canadian Standards Association, Rexdale, Ontario, 214 p.

Canadian Standards Association (CSA). (2012). "Design and construction of building components with fibre-reinforced polymers." CSA S806-12, Canadian Standards Association, Rexdale, Ontario, 177 p.

NBCC. (2010). "National Building Code of Canada." National Research Council of Canada, Ottawa, Ontario, 1167 p.

Pultrall Inc. (2102). "V-ROD^{TM}, Technical Data Sheet". ADS Composites Group Inc. http://www.pultrall.com,Thetford Mines, Quebec, Canada.

Sharbatdar, M. K. and Saatcioglu, M. (2004). "Behavior of FRP reinforced concrete under cyclic loading." 13^{th} Int. Conf. on Earthquake Engineering, (WCEE-04), Vancouver, British Columbia, Canada.

Tavassoli, A., Liu, J. and Sheikh, S. (2015). "Glass fiber-reinforced polymer-reinforced circular columns under simulated seismic loads." ACI Structural Journal, 112(10): 103-114.